electronics

MDPI

Article

Implementation and Review of the Axisymmetric Equilibrium System of RFX-Mod2 within the MARTe2 Framework

Nicolò Ferron [1,2], Claudio Finotti [2], Gabriele Manduchi [2], Giuseppe Marchiori [2], Paolo Bettini [2,3,*], Domenico Abate [2] and Roberto Cavazzana [2]

[1] Centro Ricerche Fusione (CRF), Università di Padova, Corso Stati Uniti 4, 35127 Padova, Italy
[2] Consorzio RFX (CNR, ENEA, INFN, Università di Padova, Acciaierie Venete SpA), Corso Stati Uniti 4, 35127 Padova, Italy
[3] Dipartimento di Ingegneria Industriale (DII), Università di Padova, Via Gradenigo 6/a, 35131 Padova, Italy
* Correspondence: paolo.bettini@unipd.it

Abstract: A major refurbishment of the toroidal complex of the RFX-mod device is in progress and it will include the removal of the Inconel vacuum vessel and a modification of the stainless steel supporting structure to be made vacuum-tight. The axisymmetric equilibrium control in RFX-mod was responsible for the control of the plasma current, horizontal and vertical position along with its stability and the plasma shape. The new implementation framework, both hardware and software, is described. The system has been fully reviewed and modified, if needed, for its prospective use in RFX-mod2. In order to run tests in an operation-like context, the updated system has also been implemented in the MARTe2 framework, to be deployed for the real-time applications of RFX-mod2. The results of the previous versions were reproduced and the cycle-time requirements were met.

Keywords: real time; FPGA; MARTe2; RFX-mod2

Citation: Ferron, N.; Finotti, C.; Manduchi, G.; Marchiori, G.; Bettini, P.; Abate, D.; Cavazzana, R. Implementation and Review of the Axisymmetric Equilibrium System of RFX-Mod2 within the MARTe2 Framework. *Electronics* **2022**, *11*, 2751. https://doi.org/10.3390/electronics11172751

Academic Editors: Katarzyna Antosz, Jose Machado, Yi Ren, Rochdi El Abdi, Dariusz Mazurkiewicz, Marina Ranga, Pierluigi Rea, Vijaya Kumar Manupati, Emilia Villani and Erika Ottaviano

Received: 14 July 2022
Accepted: 27 August 2022
Published: 1 September 2022

1. Introduction

RFX-mod has been operated for more than ten years as a reverse field pinch (RFP) experiment (hence its name), achieving its design performances (plasma current Ip = 2 MA and plasma temperature T = 1.5 KeV) and demonstrating the possibility of creating self-organized helical plasma discharges with increased confinement thanks to a highly effective saddle coil system for the control of the plasma modes [1]. RFX-mod relies on a real-time plasma control system, which is a fundamental component in all modern fusion devices [2–5]. The flexibility of its magnetic and power-supply system along with the mode control system allowed also the operation as a low current circular and shaped Tokamak. In order to foster the transition to improved confinement regimes (Quasi Single Helicity in RFP and H-mode in Tokamak configuration, respectively), the design of a complete refurbishment of the toroidal complex of RFX-mod has been carried out in the past years [2,6]. In particular, the aim was an upgrade of the plasma boundary conditions of the device, to be named RFX-mod2. By overcoming some intrinsic limitations of the previous versions of the device [7], RFX-mod2 should allow achieving a more complete characterization of the RFP plasma configuration up to 2 MA current and exploring a more extended set of configurations as an ohmic Tokamak. The basic change will be the removal of the Inconel vacuum vessel allowing the plasma to be closer to the highly conducting copper shell with the ratio (b/a) between the respective minor radii decreased from 1.1 to 1.04 [8,9]. The expected beneficial effects are slower growth rates of Resistive Wall Modes (RWM), reduced deformation of the last closed flux surface, increased plasma current threshold for the occurrence of Tearing Modes (TM) wall locking with associated particularly detrimental localized interactions. Beyond making it possible to obtain circular plasma with a larger cross section and correspondingly reduced resistance and loop voltage, the increased radius of the discharge chamber suggested to conduct an extended study of

new plasma shapes feasible by properly controlling the Field Shaping Coil (FSC) currents, including Tokamak discharges with $\delta > 0.3$, $\kappa > 1.5$ shape conditions and discharges with negative triangularity, as well [3,10,11]. Two examples are given in Figure 1. Moreover, the new electromagnetic measurement system [12] will allow reconstructing the plasma magnetic configuration with a higher spatial and temporal resolution, providing the full set of feedback signals needed by the magnetic control system [13]. In this context, the magnetic control system is expected to play an increasing role in creating and maintaining the larger number of desired magnetic equilibrium configurations with the required accuracy and reliably managing the transition between different configurations in the same pulse. The paper is organized as follows: in Section 2, the layout of the system is described. In Section 3, a comprehensive description of the updated version of the axisymmetric magnetic control system is given, highlighting the strong interaction among the different elements dedicated to the control of all the parameters relevant to the different envisaged scenarios. In Section 4, a new implementation of the real-time plasma control system is presented using updated hardware, as well as a new version of the software framework.

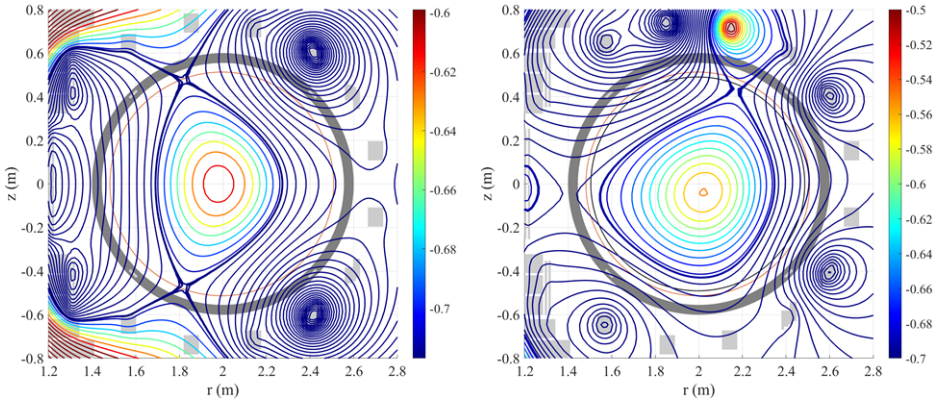

(**a**) (**b**)

Figure 1. (**a**) Double Null D-like shape with $\delta = \delta u = \delta l = 0.49$. (**b**) Upper Single Null shape with $\delta = -0.35$ ($\delta u = -0.54$, $\delta l = -0.15$).

2. System Implementation

The Plasma Control System (PCS) will be deployed on a multicore server with 64 cores. This choice is dictated by the experience gained with the previous versions of the plasma system. Indeed, the system was originally implemented as a network of computers, each carrying out a given function and exchanging data in real time via Ethernet. Using such a configuration, network communication proved to represent the system bottleneck, limiting the overall control rate to 2 kHz. For this reason, the subsequent version adopted a multicore server, where each core hosted a function formerly implemented by a separate computer [14]. In this case, the conceptual parallel and distributed nature of the system is retained, but component communication is now much faster, being carried out over distributed memory. In this way, it has been possible to increase the overall control rate to 5 kHz. Memory-based communication within a single computer is much faster than network communication, even on an insulated, high-speed 10 GB Ethernet. While in network communication, the time required to exchange a small packet of data is in the order of few tens of microseconds, due to the driver access to network cards, interrupt and stack management, the worst-case communication time in shared memory communication (i.e., cache miss and possible bus contention) is typically in the order of 10–100 ns. Communication is nevertheless required in order to let sensors and actuators communicate with the central server. For actuators, RFX-mod2 will retain the solution adopted in RFX-mod, i.e., Digital-to-Analog (DAC) devices connected via fiber optic PCI-e to the central server, and used to generate the reference waveforms to the Power Supplies for the Field Shaping

Magnetizing and Toroidal windings (8 + 1(x4PCAT) + 1(x12TCAT) signals), and for the 192 saddle coils for the control of the plasma modes.

A novel approach is adopted in RFX-mod2 for the sensors (approx. 1500 signals from Electromagnetic probes), no longer using analog integrators to derive the magnetic fields from measured magnetic flux derivatives. Direct and integrated channels for every EM probe will now be acquired by a single Analog-to-Digital (ADC) channel at high sampling speed, carrying out FPGA-based digital integration [14], as shown in Figure 2. In order to reduce the drift in integration due to signal offset, autozero offset correction is performed by the FPGA just before starting digital integration during the plasma discharge. In order to avoid possible aliasing due to subsampling for streamed data, Cascaded Integrator–Comb (CIC) low-pass filtering is performed in the FPGA before subsampling the signals to be streamed. The same FPGA will supervise high-speed data acquisition (up to 1 MHz) and subsampled data streaming (up to 10 kHz) over Ethernet towards the plasma control server.

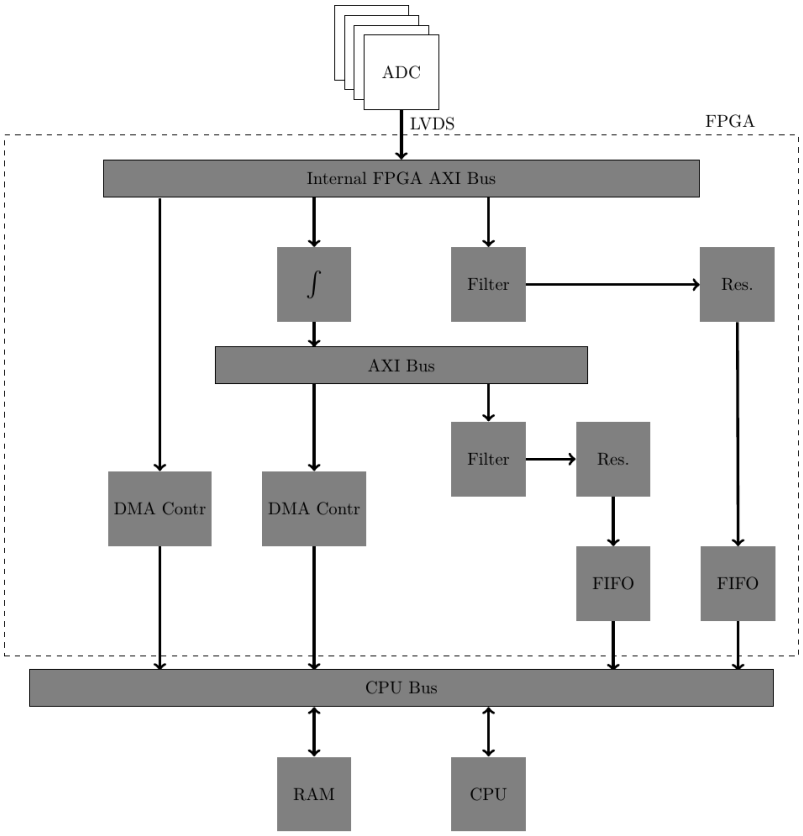

Figure 2. The FPGA architecture.

The MARTe2 framework [14,15] will be used as a wrapper for the Axisymmetric Control System (see Section 3) and for interfacing its input and output signals with sensors and actuators. The axisymmetric system inputs and outputs are listed in Tables 1 and 2, respectively.

Table 1. List of the inputs to the axisymmetric system.

	Input		Unit
1	Toroidal loop voltage	V_ϕ	V
2	Poloidal loop voltage	V_θ	V
3	Toroidal flux	Ψ_ϕ	Wb
4	Poloidal flux	Ψ_θ	Wb
5	Toroidal current	I_ϕ	A
6	Toroidal current derivative	$\dot{I}_\phi$	A/s
7	Poloidal fields	$\mathbf{B}_\theta$	T
8	Magnetizing Windings Currents	$\mathbf{I}_{MW}$	A
9	Field Shaping Coil Currents	$\mathbf{I}_{FS}$	A

Table 2. List of the outputs of the axisymmetric system.

	Output		Unit
1	MW voltage reference	$V_{MW\text{ref}}$	V
2	FSW voltage references	$\mathbf{V}_{FS\text{ref}}$	V
3	Saddle Coil current reference	$I_{SC\text{ref}}$	V

3. Description of the Axisymmetric Control System

The magnetic control system is structured as a set of interacting blocks dedicated to the control of either electromagnetic quantities such as the plasma current and the magnetic field components, or geometrical quantities such as the plasma horizontal and vertical position, the plasma section ellipticity and triangularity, the distances (gaps) of the plasma boundary from the first wall along fixed directions. These blocks are complemented by other elements performing monitoring and safety-related tasks. A global view of the system is shown in Figure 3. The system is composed of three main elements: the plasma current control block, generating the voltage reference for the magnetizing windings required to follow the preset current reference, the plasma position control block, generating the current references for the field shaping coils required to maintain the desired plasma position, and the plasma shape block, acting on plasma ellipticity and triangularity. In addition to the measured inputs of Table 1, the inputs include reference signals whose waveforms are programmed during the parameter setting stage of the pulse according to the desired characteristics of the shot and feedback signals. These are either directly measured quantities or derived quantities such as the geometrical quantities, obtained from the electromagnetic signals by using properly developed algorithms. All the measures undergo a conditioning stage to remove offset, drift, noise before being sent to the system. Output signals are voltage and current references for the power supplies feeding the coils of the electromagnetic poloidal field system and the saddle coils system mounted onto the outer surface of the stainless steel toroidal support structure. An effort was made to create a unified scheme to manage the whole operational range of the device with the aim of increasing the maintainability and reusability of the code. When the control task must be differentiated according to the selected configuration, the corresponding element of Figure 3 includes specialized functions which are enabled by setting proper flag signals in the pulse programming stage. Some examples will be given in the description of the main blocks of the control system.

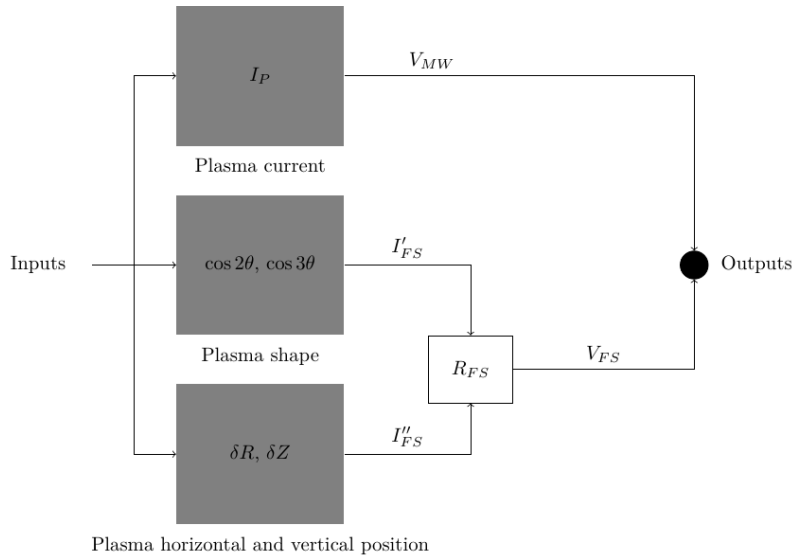

Figure 3. Block scheme of the axisymmetric magnetic control system.

3.1. The Plasma Current Control

This control produces a single voltage reference for its exclusive group of actuators, i.e., the 4 power supplies (PCAT) which apply the flat-top voltage to the 4 transfer resistances of the poloidal field electric circuit of the machine. The dynamic evolution of the 4 Magnetizing Winding (MW) sector currents and the associated flux linked with the plasma ring are driven so as to control the plasma current. Input signals are also the loop voltage and the plasma current derivative. They are used in dedicated blocks for the real-time calculation of the plasma resistance and the ohmic power, which are then transmitted to the RFP plasma current control block, the former as a basic information to optimize the plasma current control, the latter as a monitored quantity to command a possible controlled voltage ramp-down. Other input signals are the currents of the 4 Magnetizing Winding sectors and the 8 Field Shaping Coils (FSC): they are needed to perform real-time calculations of the associated resistive voltage drops in the electric circuit corresponding to the flat-top phase of the pulse. These estimated resistive voltage drops are added to a programmable voltage reference signal to create the feedforward component, which is distributed to both RFP and Tokamak current control functions. The voltage reference feedback component is produced by a simple proportional controller in the Tokamak case and by a lead lag compensator in the RFP case.

3.2. The Control of Horizontal Position and Shape by FSC Currents

The plasma horizontal position control and the plasma ellipticity and triangularity control have the same actuators, i.e., the 8 independently controlled FSC power-supplies, and their outputs are 8 FSC current references which are then converted into 8 voltage references by the cascaded FSC current control block. Together with the vertical position control, whose actuators are different, as it will be explained later, they are used both in limiter and Single/Double Null discharges. In fact, beyond the basic control of plasma equilibrium, the plasma boundary can be shaped to some extent by the independent control of the plasma center position, plasma section ellipticity and triangularity (another, more integrated, approach to the control of the plasma shape has also been implemented and will be described in Section 3.4). The FSC current references produced by the three SISO (Single-Input, Single-Output) control systems are then summed and the result is fed to the cascaded FSC current control block, while the control of the vertical position and its stability are independently ensured by the corresponding control system. All the controlled geometric quantities, i.e., the feedback signals, are obtained by calculating the Fourier harmonic components of the discrete function $r(\theta_i)$, which represents the distance of the plasma boundary from the discharge chamber center along the i-th sensor angle θ_i. The

function $r(\theta_i)$, in turn, is the output result of an algorithm processing the available measures of the magnetic field Br and Bp components and poloidal flux Ψ_θ.

3.2.1. The Plasma Horizontal Position Control

The control of the plasma horizontal position is performed as the control of the plasma horizontal shift δR with respect to the center of the discharge chamber, the position of the shell center is the same as that of the removed vessel since they have the same major radius R = 1.995 m. The plasma shift is calculated as the 1st $\cos\theta$ harmonic of $r(\theta)$. It must be pointed out that since each pulse is initially a circular discharge, this block is activated either throughout the whole pulse or at least in a part of it. The control system consists of a feedforward block and a feedback block. Both blocks contain specialized functions corresponding to the operating scenario: circular/shaped plasma with full set of connected FS coils (typically RFP/limiter Tokamak discharge) and circular + shaped Single/Double Null plasma with reconfigured/reduced set of FS coils. The required scenario is activated as usual by proper flags. The purpose of the feedforward block is to produce an array of FSC current references to create the required equilibrium vertical component of the magnetic field and the total m.m.f. to compensate the plasma m.m.f. The two tasks have been decoupled by calculating two FSC current distributions, the former to produce the required m.m.f. with minimum magnetic field inside the winding and the latter to produce, conversely, the required vertical field component inside with minimum total m.m.f. The feedforward vertical field reference $B_{V\mathrm{refFF}}$ is the theoretic equilibrium field depending on the planned discharge parameters and proportional to the plasma current. After multiplying the signal by a proper gain, the component of the feedforward B_V signal is obtained. The resulting feedforward $B_{V\mathrm{ref}}$ is finally transformed into 8 FSC current references again according to a set of fixed coefficients. The case of circular+shaped discharge with reconfigured FS coils is a bit more complicated because the possibility of achieving the same decoupling as in the standard configuration used for circular plasma discharges is not ensured. Moreover, the two arrays of coefficients used to transform the $B_{V\mathrm{ref}}$ signal and the m.m.f. reference signal into two arrays of FSC current references in the circular phase are different from those in the shaped phase. Thus other transition blocks are present to manage the switch between the references always by means of time linear varying factors. The feedback block also includes a version to be enabled for the circular/shaped plasma with full set of connected FS coils and another to be enabled for the circular+shaped Single/Double Null plasma with reconfigured/reduced set of FS coils. The main difference concerns the management of the horizontal shift reference. In the standard FSC configuration for circular discharges, the reference signal programmed waveform is directly fed to the summing node where the difference with the real-time calculated shift is taken. On the contrary, in the version for reconfigured FS Coils with transition from circular to shaped discharge, the requirement of changing the horizontal reference signal used in the circular phase to a new one consistent with the plasma shape control must be fulfilled. To this purpose, the array of gap references $g_{i_{\mathrm{ref}}} = r_{i_{\mathrm{ref}}} - r_{\mathrm{wall}}$ has been added as a further input signal, where $r_{i_{\mathrm{ref}}}$ is the reference radial position of the plasma surface at the i-th angle and r_{wall} is the radial position of the wall. The horizontal shift reference can then be obtained as

$$\delta R_{\mathrm{ref}} = \frac{2}{N}\sum_{i}^{N} r_{i_{\mathrm{ref}}}\cos\theta_i = \frac{2}{N}\sum_{i}^{N} g_{i_{\mathrm{ref}}}\cos\theta_i. \quad (1)$$

The usual linear transition factor allows the bumpless switch from the shift reference of the circular phase to the shift reference of the following shape control phase.

A common feature of the two versions is the PI regulator which processes the position error and generates the corresponding feedback correction $B_{V\mathrm{refFB}}$ of the vertical field request. Finally, the signal $B_{V\mathrm{ref}}$ is transformed into an array of 8 FSC current references. Again, the linear transition factor is applied between the references obtained with the

two different arrays of sharing coefficients used in the two discharge phases with the reconfigured/reduced set of FS coils.

3.2.2. The Plasma Ellipticity and Triangularity Control

According to the above mentioned definition of the plasma boundary geometric parameters, ellipticity and triangularity are expressed as the 2nd and 3rd Fourier harmonic components of the function $r(\theta)$, respectively, where $r(\theta)$ is the distance of the plasma boundary from the discharge chamber center. In particular, the reference and the feedback signals are always here understood as the required and measured $\cos 2\theta$ and $\cos 3\theta$ harmonic coefficients of $r(\theta)$, respectively. This corresponds to consider only plasmas with horizontal/vertical ellipticity and outward/inward pointing triangularity, or their combination. The basic architecture of these two control systems is similar to the previous one: a feedforward block and a feedback one process the input signals in parallel and produce two arrays of FSC current references, which are then summed and delivered as output signals. The two control systems are enabled by a dedicated block when both the plasma current is larger than a prescribed minimum value and the time is within a prescribed interval. The outputs of the two blocks are then summed and the resulting reference of either the $\cos 2\theta$ or the $\cos 3\theta$ harmonic component of the FSC currents is limited within two symmetric values and finally transformed into an array of current references for the eight coils of the FSW.

3.2.3. The FSC Current Control

The total FSC current references are eventually obtained by summing the outputs of the plasma position, ellipticity and triangularity control systems with the additional FSC current references present in the signal input array. The FSC current control block converts the input FSC current references into 8 voltage references for the FSC power supplies. The aim is to obtain an equalized dynamic response of the single FSC currents so as to maintain the fixed distribution among the coils as accurately as possible. A compensation of the resistive voltage drops was introduced to simulate a system made up of ideally conducting coils. A state feedback matrix was evaluated to diagonalize the system and to allocate its eigenvalues. A common time response of about 20 ms for the fully decoupled system was achieved.

3.3. The Plasma Vertical Position Control by Saddle Coil Currents

Similarly to the horizontal position case, the control of the vertical position is performed as the control of the plasma vertical shift δZ with respect to the discharge chamber center, which means that the shift reference and feedback signal are the required and measured Fourier $\sin\theta$ harmonic component of the function $r(\theta)$, respectively. Vertical position instability is not an issue in the standard RFP circular discharges, but the extension of the operational scenario to elongated or Single/Double Null Tokamak discharges required designing a controller able to stabilize the vertical equilibrium, as well. Due to the connection of the FSCs and the need of a faster response, the generation of the required horizontal component of the magnetic field is committed to the outer and inner array of saddle coils (the ones across the equatorial plane) out of the full set of 4 toroidal arrays, each consisting of 48 coils, in all 192 coils independently fed and completely covering the outer surface of the toroidal support structure. Although the saddle coils make up a discrete system both toroidally and poloidally, this control can still be considered axisymmetric since its output is the reference $m = 1$, $n = 0$ $\cos\theta$ component of the saddle coil current distribution, where m and n are the poloidal and toroidal harmonics of the 2D Fourier series. The control of that component is equivalent to feeding a single virtual coil obtained by the series connection of the outer array with the antiseries connection of the inner array. Beyond the usual presence of the feedforward block and feedback block, this system includes dedicated parts to manage the transition from circular to Single/Double Null Tokamak discharges and between the control systems operating in the different phases of the discharge. A block

allows a time linear dependent switch from a preprogrammed, vertical shift reference to another reference which is obtained by calculating the $\sin\theta$ harmonic of the programmed gap reference $g_{i_{\mathrm{ref}}}$ valid in the shaped plasma discharge phase. As in the horizontal shift case (see Equation (1)), it can be written:

$$\delta Z_{\mathrm{ref}} = \frac{2}{N}\sum_{i}^{N} g_{i_{\mathrm{ref}}} \sin\theta_i. \tag{2}$$

No switch is needed for the feedback signal since in RFX, it is always calculated as

$$\delta Z = \frac{2}{N}\sum_{i}^{N} r(\theta_i)\sin\theta_i = \frac{2}{N}\sum_{i}^{N} g_i \sin\theta_i. \tag{3}$$

The feedback block consists of a PID regulator that has the same structure as those used in the other control systems, in particular, filtered derivative component and saturated, independently activated integral component are present. Two alternative different paths are possible for the PID output. It can be either directly fed through, in the case of standard circular discharges, or processed by a further inner block, which handles the switch between two different vertical shift feedback control signals in the case of Single/Double Null discharge. In this second phase of the discharge, the problem of instability typically arises and a controller with different parameters could be needed. Since linearized models of the RFX-mod plasma response in Tokamak SN/DN plasma discharges had been worked out, a full model-based approach to the controller design was followed and the vertical shift control loop was nested inside a Linear Quadratic Gaussian (LQG) controller (see Section 3.4) of the plasma shape [16]. The output of this controller, properly designed to stabilize the plasma vertical position, is added (in a summing node) to a base value corresponding to the output of the above mentioned PID controller sampled at the start of the LQG shape control. In the experimental scenarios considered up to now, a simple proportional controller was sufficient to achieve this goal.

Finally, the outputs of the feedforward and feedback blocks are summed to obtain the SC current reference, which is sent to the power-supply local control after being limited within a fixed percentage of the maximum rated current of the SC power-supplies.

3.4. The Plasma Shape LQG Control

The plasma shape LQG control system is shown in Figure 4. The LQG system uses the array of gap references as input and generates FSC voltage references used as an alternative to the references generated by the feedback system of the FSC currents. The presence of a conducting shell, the highly coupled poloidal field system and the relatively low voltage limits suggested the development of a fully model-based feedback system based on a LQG scheme to deal with these aspects at the same time by only defining a set of gap references for the system. An advantage of this method is defining in a single step the overall plasma scenario, in respect of tuning each single component of the axisymmetric system (as described in Sections 3.1–3.3). As anticipated in the previous section, CREATE-L linearized models of the plasma response [16,17] were developed for typical Single Null/Double Null Tokamak equilibria in RFX-mod having FSC (8) and SC (1) voltages as input signals and the 8 plasma-wall gaps among the output signals. The control system was designed on the basis of a standard state-space representation of the LTI model of the plasma response, where all the quantities must be understood as variations with respect to the equilibrium values:

$$\dot{x}(t) = Ax(t) + Bu(t) \tag{4}$$

$$y(t) = Cx(t) + Du(t) \tag{5}$$

The states are associated to the currents in the active and passive conductors of RFX-mod. Due to the presence of toroidal complex structures, their number is relatively high

(more than 180) and the constraints of the real-time implementation suggested to obtain a reduced-order model by standard techniques. The LQG controller was then designed, consisting of a Kalman plasma state estimator and a Linear Quadratic optimal gain matrix [16]. Feedforward terms and an integral action were added to improve the system performances and capability to follow the reference signals with the desired accuracy. While the general architecture does not have to be modified, the choice of the controller parameters depends on the considered equilibrium. In RFX-mod, the final tuning was accomplished during dedicated experimental campaigns. The output of the control system is an array of 8 voltage references for the FS coils (VFS), the reference for the SC power supply being produced by the vertical position control inner loop.

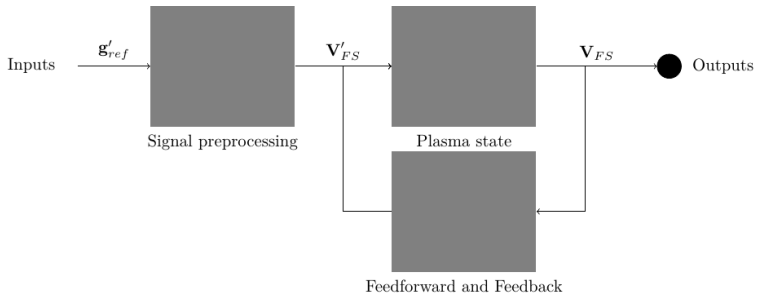

Figure 4. Block scheme of the plasma shape LQG control system.

The control system has been designed to follow the required, even if relatively limited, variations of the gap references. This, in turn, implies calculating the matrices converting the gap references into voltage and state references. Due to ill-conditioning of these matrices, the occurrence of generating voltage requests beyond the deliverable values appeared frequently in the preliminary simulations when the typical programmed gap references were directly applied, entailing the nonlinear operation of the control system at the saturation limits. In order to overcome this issue, a model-based, real-time modification of the gap references was implemented by exploiting a SVD decomposition of the static matrix relating the gap array to the voltage array. The removal of the gap reference components associated to the highest singular values proved to allow extending the range of linear operation without significant variations in gap references.

A Kalman filter has been implemented in a standard state-space representation. The set of state-space model matrices can be chosen in the pulse parameter setting phase out of four preloaded different sets corresponding to different values of the covariance matrices of plant disturbances and input noise signals assumed in the design. This has been particularly useful since the first commissioning of the system to speed up the performance optimization phase. The Kalman filter input signals are the measured gap difference array, the FSC current difference array and the voltage reference difference array, the plasma vertical shift and its reference, calculated according to the above-mentioned definition from the measured gap and gap reference difference arrays. In particular, the SVD-filtered version of the gap reference difference array is used. The output signals are the one-step updated Kalman estimates of gaps, FSC and plasma currents, plasma vertical shift and states of the reduced-order model.

The references of the FSC voltage differences are obtained as the sum of a feedforward and a feedback component. The feedforward component is directly obtained by a model-derived matrix converting the gap difference vector to a FSC voltage difference vector. The feedback component consists of an integral term of the gap error $\int K_t(\mathbf{g}_{\text{ref}} - \mathbf{g})dt$ and a state error feedback term $K_{LQ}(\mathbf{x}_{\text{ref}} - \mathbf{x})$, where $\mathbf{x}$ is the state vector of the LTI system.

The final absolute FSC voltage references are obtained by summing the above mentioned contributions to the baseline value sampled at the start of the LQG control.

4. Implementation in the New MARTe2 Framework

The axisymmetric system has been implemented in a test framework so as to verify its functionality in view of future operations. The system is inserted in MARTe2 [14,15], a fusion framework adopted by several fusion experiments [18]. The final system is in fact expected to be run using MARTe2. To do so, a dedicated wrapper component has been developed that interfaces with the axisymmetric equilibrium system, providing it with the input values taken from the diagnostics and sending its output values to the other components of the system, such as the power-supply control units. In order to perform an off-line test of the system, the framework was set up to use experimental data from previous discharges.

The system was then run and its outputs were compared with the expected outputs so as to verify the system applicability and performances. The results are shown in Figures 5 and 6.

The performed tests addressed two aspects: output accuracy, i.e., making sure that exactly the same numeric results are obtained in the new implementation in respect of the former system, and cycle timing, i.e., making sure that the worst-case execution time (WCET) of the algorithms in the new implementation is compatible with the expected control cycle frequency (10 kHz) in the new system. Output accuracy was achieved, as shown in Figures 5 and 6, where the control algorithm outputs in the new system are coincidental with those from the previous system. Cycle timing was proven to be satisfactory by measuring computation time and jitter in the new MARTe2 framework, as shown in Figure 7. The control computation WCET can be safely assumed to be 20 µs, and even considering WCET for the other control chain components (i.e., communication, ADC and DAC conversion), the overall cycle computation time is shorter than the target 100 µs cycle time.

The system is, therefore, working as expected by generating the correct voltage references for the FSC and the current reference for the Saddle Coil System. In particular, no difference has been observed with previous versions of the model and the cycle time is below the requirements of the RFX-mod2 PCS.

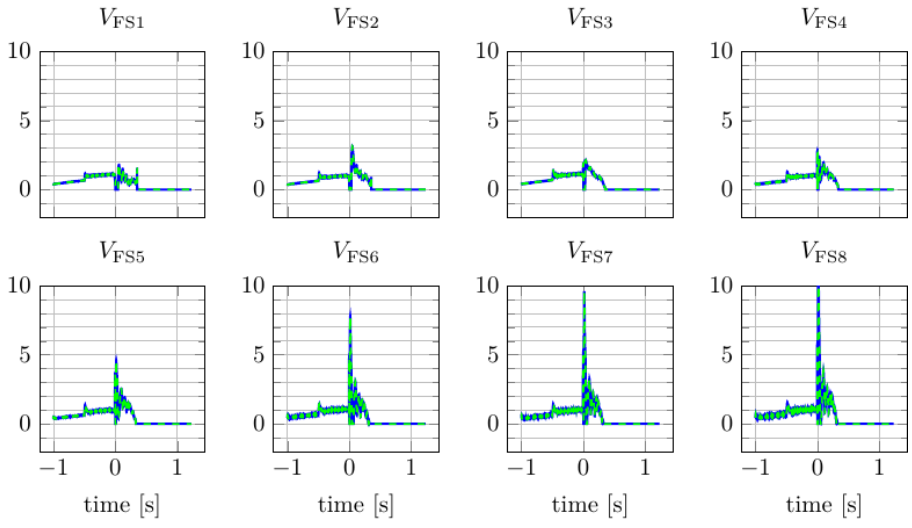

Figure 5. Voltage references of the Field Shaping Coils [V] produced by the reviewed axisymmetric system (dashed) obtained by feeding the system with waveforms from previous experiments compared with the experimental outputs. Voltage values are scaled to a factor of 150.

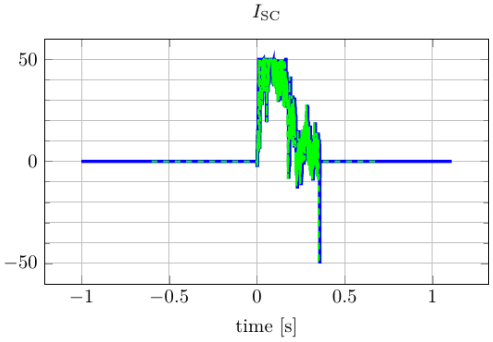

Figure 6. Current reference of the Saddle Coil [A] produced by the reviewed axisymmetric system (dashed) obtained by feeding the system with waveforms from previous experiments compared with the experimental outputs.

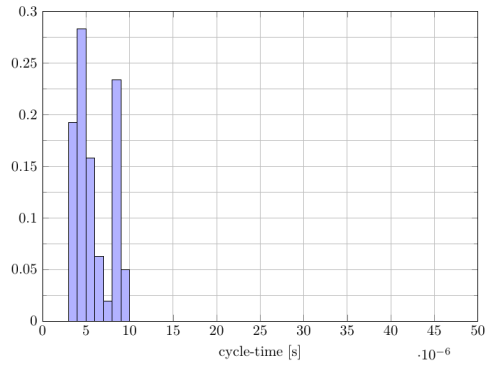

Figure 7. Relative frequency of cycle times of the equilibrium and shape system over 10,000 cycles. WCET is 10 µs.

5. Conclusions

In this work, a fully reviewed version of the axysimmetric equilibrium control system of RFX-mod is presented, highlighting its components, such as the horizontal position, vertical position and shape elements. The previous distinct modules developed for circular discharges and Single/Double Null discharges, respectively, were merged into only one flexible system. An effort was also made to update the control system for its prospective use in refurbished version of the experiment, named RFX-mod2. To run tests in an operational context, the control system was integrated in the new S/W framework MARTe2, which will be used for all the real-time control applications in RFX-mod2. Promising results have been obtained in terms of both accuracy and cycle-time performances by comparison with the previous versions, thus confirming that the axisymmetric equilibrium system of RFX-mod, with the proposed modifications, is ready to be applied to RFX-mod2.

Author Contributions: Conceptualization, N.F. and G.M. (Giuseppe Marchiori); methodology, G.M. (Giuseppe Marchiori); software, C.F., G.M. (Giuseppe Marchiori), R.C. and N.F.; validation, C.F., G.M. (Giuseppe Marchiori), G.M. (Gabriele Manduchi), R.C. and N.F.; writing—original draft preparation, G.M. (Giuseppe Marchiori) and N.F.; writing—review and editing, P.B. and G.M. (Gabriele Manduchi); visualization, N.F., D.A., G.M. (Giuseppe Marchiori) and G.M. (Gabriele Manduchi); supervision, P.B., G.M. (Gabriele Manduchi) and G.M. (Giuseppe Marchiori). All authors have read and agreed to the published version of the manuscript.

Funding: This research received no external funding.

Institutional Review Board Statement: Not applicable.

Informed Consent Statement: Not applicable.

Data Availability Statement: Not applicable.

Conflicts of Interest: The authors declare no conflict of interest.

References

1. Marrelli, L.; Abate, D.; Agostinetti, P.; Agostini, M.; Aprile, D.; Auriemma, F.; Berton, G.; Bettini, P.; Bigi, M.; Boldrin, M.; et al. Status of the RFX-Mod2 upgrade. In Proceedings of the 28th IAEA Fusion Energy Conference, Virtual, 10–15 May 2021.
2. Marrelli, L.; Cavazzana, R.; Bonfiglio, D.; Gobbin, M.; Marchiori, G.; Peruzzo, S.; Terranova, D. Upgrades of the RFX-mod reversed field pinch and expected scenario. *Nucl. Fusion* **2019**, *59*, 076027. [CrossRef]
3. Ambrosino, G.; Albanese, R. Magnetic control of plasma current, position, and shape in Tokamaks: A survey or modeling and control approaches. *IEEE Control Syst.* **2005**, *25*, 76–92.
4. Castaldo, A.; Albanese, R.; Ambrosino, R.; Crisanti, F. Plasma Scenarios for the DTT Tokamak with Optimized Poloidal Field Coil Current Waveforms. *Energies* **2022**, *15*, 1702. [CrossRef]
5. De Tommasi, G. Plasma Magnetic Control in Tokamak Devices. *J. Fusion Energ.* **2019**, *38*, 406–436. [CrossRef]
6. Peruzzo, S.; Agostini, M.; Agostinetti, P.; Bernardi, M.; Bettini, P.; Bolzonella, T.; Zanotto, L. Design concepts of machine upgrades for the RFX-mod experiment. *Fusion Eng. Des.* **2017**, *123*, 59. [CrossRef]
7. Lunardon, F.; Maistrello, A.; Gaio, E.; Piovan, R. Feasibility study of RFX-mod2 performance improvement by additional magnetic energy storage. *Fusion Eng. Des.* **2021**, *173*, 112791. [CrossRef]
8. Dalla Palma, M.; Berton, G.; Canton, A.; Cavazzana, R.; Gambetta, G.; Innocente, P.; Spolaore, M. Design of the RFX-mod2 first wall. *Fusion Eng. Des.* **2020**, *160*, 111795. [CrossRef]
9. Berton, G.; Bernardi, M.; Dalla Palma, M.; Marcuzzi, D.; Pavei, M.; Peruzzo, S. Design of the new supporting structure for the passive stabilizing shell assembly of RFX-mod2. *Fusion Eng. Des.* **2021**, *169*, 112466. [CrossRef]
10. Abate, D.; Marchiori, G.; Bettini, P.; Villone, F. Modelling of RFX-mod2 tokamak equilibria with DEMO-like shape conditions and negative triangularity. *Plasma Phys. Control. Fusion* **2020**, *62*, 085001. [CrossRef]
11. Abate, D.; Marchiori, G.; Villone, F. Modelling and experimental validation of RFX-mod Tokamak shaped discharges. *Fusion Eng. Des.* **2019**, *146*, 135–138. [CrossRef]
12. Marconato, N.; Cavazzana, R.; Bettini, P.; Rigoni, A. Accurate Magnetic Sensor System Integrated Design. *Sensors* **2020**, *20*, 2929. [CrossRef] [PubMed]
13. Marconato, N.; Bettini, P.; Cavazzana, R.; Grando, L.; Marchiori, G.; Marrelli, L.; Pomaro, N. Design of the new electromagnetic measurement system for RFX-mod upgrade. *Fusion Eng. Des.* **2019**, *146*, 906–909. [CrossRef]
14. Manduchi, G.; Luchetta, A.; Taliercio, C.; Rigoni, A.; Martini, G.; Cavazzana, R.; Ferron, N.; Barbato, P.; Breda, M.; Capobianco, R.; et al. The upgrade of the control and data acquisition system of RFXMod2. *Fusion Eng. Des.* **2021**, *167*, 112329. [CrossRef]
15. Manduchi, G.; Fredian, T.W.; Stillerman, J.A.; Neto, A.; Sartori, F. Fast development of real-time applications using MDSplus and MARTe frameworks. *Fusion Eng. Des.* **2016**, *112*, 942–945. [CrossRef]
16. Marchiori, G.; Finotti, C.; Kudlacek, O.; Villone, F.; Zanca, P.; Abate, D.; Marrelli, L. Design and operation of the RFX-mod plasma shape control system. *Fusion Eng. Des.* **2016**, *108*, 81–91. [CrossRef]
17. Albanese, R.; Villone, F. The linearized CREATE-L plasma response model for the control of current, position and shape in tokamaks. *Nucl. Fusion* **1998**, *38*, 723. [CrossRef]
18. Manduchi, G.; Luchetta, A.; Taliercio, C.; Rigoni, A.; Sartori, F.; Neto, A.; Carannante, G. A portable control and data acquisition solution using EPICS, MARTe and MDSplus. *Fusion Eng. Des.* **2018**, *127*, 50–53. [CrossRef]